Allelotypes and Fluorescence *In situ* Hybridization Profiles of Poorly Differentiated Endocrine Carcinomas of Different Sites

Daniela Furlan, Barbara Bernasconi, Silvia Uccella, Roberta Cerutti, Ileana Carnevali, and Carlo Capella

Department of Human Morphology, Anatomic Pathology Unit, University of Insubria, Varese, Italy

ABSTRACT

Purpose: **The aim of this work was to investigate the genotypic profiles of 36 poorly differentiated endocrine carcinoma (PDEC) of different sites to verify if their very similar phenotype may reflect similar pattern of genetic anomalies and if useful diagnostic or prognostic markers may be pointed out.**

Experimental Design: **All tumors were microallelotyped at 57 microsatellite on 11 autosomes and the allelotypes of a selected panel of tumors were validated by interphasic fluorescence *in situ* hybridization with centromeric probes for chromosomes 1, 3, 6, 11, 17, and 18 and a probe specific for *p53*.**

Results: **Regardless of the primary sites, PDECs exhibit very complex allelotypes (86%) and *TP53* allelic imbalance (89%). Among these cases, fluorescence *in situ* hybridization analysis confirmed the presence of multiple aneusomies and a chromosome instability phenotype. Very low percentage of allelic imbalance (AI) and few aneuploidies were detected in only five PDECs for which an overall longer survival was observed. We found recurrent AI on 3p, 5, and 11q13 in lung PDECs, on 5q21, 8p, and 18q21 in colorectal PDECs and on 7 and 11q22 in gastric PDECs. Significantly better outcome was observed in patients with PDEC exhibiting 8q AIs and absence of AI at chromosome regions 6q25 and 6p.**

Conclusions: **The concurrence of p53 inactivation and aneuploidies or chromosome instability are the main features of PDECs. However, the specific allelotypes observed in relation to primary site support the hypothesis that PDECs and exocrine carcinomas of all sites may share early pathogenetic mechanisms. Molecular markers of potential diagnostic and prognostic values for PDECs of different sites have been identified.**

Received 8/26/04; revised 12/1/04; accepted 12/8/04.

Grant support: University of Insubria and Fondazione Cariplo, Varese, Italy.

The costs of publication of this article were defrayed in part by the payment of page charges. This article must therefore be hereby marked *advertisement* in accordance with 18 U.S.C. Section 1734 solely to indicate this fact.

Requests for reprints: Daniela Furlan, Department of Pathology, Ospedale di Circolo Viale Borri, 57 21100, Varese, Italy. Phone: 39-0332264557; Fax: 39-0332262313; E-mail: daniela.furlan@uninsubria.it.

INTRODUCTION

Poorly differentiated endocrine carcinoma (PDEC) is a poorly differentiated neoplasm with an aggressive biological behavior and a very negative outcome (1). The morphologic diagnosis of PDECs relies on the recognition of a proliferation of highly atypical cells, varying in size from small to large, showing a prominent mitotic and apoptotic activity and, frequently, large areas of necrosis. The immunohistochemical analysis of general endocrine markers in neoplastic cells is crucial for the differential diagnosis of a PDEC as opposed to other nonendocrine poorly differentiated carcinomas. PDEC of the lung, including both small cell carcinoma and large cell neuroendocrine carcinoma, is by far the most common type of PDEC, representing up to 20% of lung epithelial malignant tumors (2). However, PDECs can arise with the same morphologic features in virtually all body sites (3), sharing various features with lung PDECs such as the association with cigarette smoking, a similar tumor biology and an apparent chemosensitivity.

Extrapulmonary PDEC has been increasingly recognized as a distinct nosologic entity, although it still represents a diagnostic and therapeutic problem and is often confused with metastatic lung PDEC (4–7). In clinical practice, extrapulmonary PDEC is currently treated in a similar way to lung PDEC and it has been shown responsive to commonly employed radiotherapeutic and chemotherapeutic regimens. However, like its pulmonary counterpart, clinical and pathologic remission is short-lived and the outcome remains very poor, with an overall survival of a few months (6, 8).

The histogenesis of PDECs is still controversial. One hypothesis is that the clinicopathologic similarities of these tumors may reflect a common cell origin, presumably from a multipotent cell of the diffuse endocrine system. This model suggests a common ancestral cell derived from neural crest which migrates to various epithelial sites throughout the body. However, embryologic evidence for this hypothesis is lacking (3, 4). An alternative hypothesis is that the cell of origin is an endodermally derived stem cell that can result in endocrine and exocrine differentiation (3, 4). This would account for the frequent admixtures in these tumors of cell types with multilinear differentiation and for the existence of rare mixed exocrine/endocrine tumors where an adenomatous and/or carcinomatous component is associated with a PDEC. In these mixed tumors, a close genetic relationship between the endocrine and the exocrine components has been shown, supporting the hypothesis of a common pathogenetic mechanism for PDECs and carcinomas from the same site (9–11). An immediate consequence of this hypothesis is that PDECs, despite similarities in histologic appearance, may be characterized by specific tumorigenic mechanisms and unique patterns of genetic alterations depending on the primary site of the tumor.

At the molecular level, there is little information about the genotypic profiles of extrapulmonary PDECs, largely because of the relatively low frequency of these tumors (9, 10, 12–14). By

contrast, intensive research on a large number of small cell lung cancers has shown very complex karyotypes with multiple numerical and structural chromosome aberrations indicative of a high degree of chromosome instability (CIN; refs. 15, 16). Despite the complexity of these alterations, recurrent chromosome gains and losses have been identified by modern cytogenetic and molecular techniques (17, 18). In agreement with the current body of literature, extensive 3p deletions have been described as a typical alteration in lung PDECs (19), whereas the same observation has not been shown in very small series of extrapulmonary PDECs (20). In addition, losses of 17p, 5q, 10q, 16q and gains of 1p, 3q, 14q have been identified as very frequent chromosomal alterations in lung PDECs (17).

The aim of this work was to carry out a microallelotyping analysis of a well-characterized series of PDECs of different sites to identify distinct patterns of genetic abnormalities with respect to the primary site of the tumor and to provide molecular markers of potential diagnostic or prognostic value. Moreover, for a selected group of PDECs, the resulting allelotypes were validated by interphasic fluorescence *in situ* hybridization (FISH) to examine the relationship between allelic imbalance (AI) and numerical chromosome abnormalities both in chromosome-stable and chromosome-unstable karyotypes.

MATERIALS AND METHODS

Patients and Samples. Thirty-six PDECs were obtained with informed consent from 36 patients who had undergone surgical or endoscopic resection. The cases were selected from the files of the Pathology Department of the Varese Hospital, which is the referral institution for a population of >200,000 individuals. A total of 857 PDECs over a period of 20 years were found, representing 4.2% of all malignant epithelial tumors of the sites analyzed, with a range comprised between <0.1% in the colon and the stomach and >14% in the lung. The PDECs were included in the study considering the availability of the normal samples of each patient and the quality of the extracted DNA (recent cases were better preserved).

The clinicopathologic features and the primary sites of the tumors are reported in Table 1. The diagnosis of PDEC was determined using histopathologic criteria and cell marker analysis according to the WHO criteria (1). The size of the primary tumors, the occurrence and the location of the metastases, the presence of necrosis and vascular invasion, the cell size and the mitotic index (number of mitotic figures in 10 high-power field ×400) were recorded for each case. Follow-up data were collected by contacting clinicians and/or by consulting the Tumor Registry of the Lombardia region (Italy).

Table 1 Clinicopathologic data of the 36 PDECs analyzed

Site	Case no.	Sex	Age	Size (cm)	Stage	Metastasis	Necrosis	Angioinvasion	Cell size	Mitosis	Ki67 (%)	Follow-up	Months
Lung	1	M	67	1.5	I	–	+	yes	I	65	37	DOD	18
	2	M	76	NA	III	Skin	+	yes	I	215	49	DOD	3
	3	M	79	8	II	LN	+++	yes	I/L	39	45	ANED	10
	4	M	69	12.5	II	LN	+++	yes	L	81	30	DOC	3
	5	M	62	2.5	II	LN	++	yes	L	111	63	ANED	8
	6	M	60	2	I	–	+	yes	S	95	65	DOD	27
Stomach	7	M	67	3	III	LN/liver	+	yes	I	39	64	DOD	12
	8	M	59	5	II	LN	+	yes	I	44	51	DOD	5
	9	M	59	5	II	LN	+	yes	I	109	70	DOD	6
	10	M	72	14	II	LN	+	yes	I	219	70	DOD	12
	11	M	62	1.2	I	–	–	yes	I	103	60	ANED	48
	12	M	37	3	II	LN	+	yes	I	173	70	ANED	11
	13	F	63	8	II	LN	+	yes	I/L	112	63	ANED	15
Colon-rectum	14	F	63	7	III	LN/Liver	+	yes	I	67	60	DOD	1
	15	F	75	4	II	LN	+	yes	I	170	65	DOD	1
	16	M	50	7	II	LN	+	yes	I/L	71	70	DOD	3
	17	M	67	4	I	–	+	yes	I	53	50	DOD	1
	18	M	62	2.5	III	LN/liver	+	yes	I/L	163	60	DOD	5
	19	M	60	5	II	LN	–	yes	I	99	60	ANED	22
	20	F	77	2.5	I	–	–	yes	I	84	40	ANED	72
	21	M	65	6	III	LN/liver	+	yes	I/L	44	70	NA	NA
	22	M	59	6.5	II	LN	–	yes	I/L	65	62	ANED	6
	23	F	58	NA	III	liver	–	NA	I	70	70	NA	NA
Esophagus	24	M	66	3	II	LN	++	yes	I/L	80	64	DOD	6
	25	M	45	5.5	III	LN/lung	++	yes	I	105	56	DOD	7
Pancreas	26	M	58	3	III	LN/liver	+	yes	S	30	27	DOD	3
Gallbladder	27	F	77	2.5	III	Liver	+++	yes	I	215	58	DOD	1
Bladder	28	M	81	4.5	NA	NA	+++	yes	I/L	59	26	DOD	28
	29	M	36	3.5	NA	NA	+	yes	I	198	60	DOD	23
	30	M	86	NA	NA	NA	+	yes	I	111	55	DOD	13
Prostate	31	M	77	3	NA	NA	–	yes	I	33	15	DOD	1
	32	M	67	NA	NA	NA	++	yes	I	100	71	DOD	3
Endometrium	33	F	64	3.5	II	LN	–	yes	L	97	25	ANED	39
Skin	34	F	68	NA	II	LN	+	yes	I	122	68	ANED	29
	35	F	51	0.8	I	–	–	no	I	110	70	ANED	38
Parotid gland	36	F	82	6	II	LN	+	yes	I/L	104	59	DOD	6

Abbreviations: ANED, alive with no evidence of disease; DOD, died of disease; DOC, died of other causes; LN, Lymph node; NA, not available; –, negative: S, small; I, intermediate; L, large.

Immunohistochemistry for the detection of general endocrine markers (synaptophysin, neuron-specific enolase, PGP9.5, and CD56), Ki67 antigen, and p53 was done as previously described (11).

Allelotyping PCR. Normal and tumor DNA of all 36 patients in Table 1 were obtained from archival paraffin-embedded specimens after a manual microdissection to enrich the neoplastic cellularity of at least 80% in all tumor samples (11). All 36 PDECs were allelotyped using a panel of 57 polymorphic markers covering a total of 26 different chromosomal regions (Table 2). Thirty of these markers are physically mapped near known TSGs or loss of heterozygosity regions reported as critical in endocrine tumorigenesis (1pq, 3p, 5q, 6q, 11pq, 17p, and 18q; ref. 14). Furthermore, all tumors were analyzed for AI on chromosomal arms 3q, 4pq, 5p, 7pq, 8pq, 10pq, 17q, and 18p using one or two microsatellite markers per arm to provide high-resolution allelotypes and to extend the analysis to chromosomes often involved in exocrine tumorigenesis (21–23).

Primers for amplification were obtained according to published sequences (http://www.gdb.org). PCR and post-PCR analysis were carried out under previously published conditions (11). An allelic imbalance, suggestive either of an allelic loss or gain, was scored by the ratio of relative allelic peak height in the tumor DNA to relative allelic peak height in the corresponding normal DNA (14). For each tumor allelotype the fractional AI (FAI) was calculated by the number of chromosomal regions having AI (AI at one or more markers within the same region were considered as unity), divided by the total number of informative chromosomal regions among the 26 analyzed (Table 2). The percentage of AI was calculated by the number of tumors showing AI in each chromosomal region (AI at one or more markers within the same region were considered as unity) divided by the total number of informative cases in that region.

Confirmation of Allelic Imbalance Data by Interphasic Fluorescence *In situ* Hybridization on Selected Cases and Criteria for Fluorescence *In situ* Hybridization Aneusomy. The allelotyping results were confirmed by interphasic FISH on eight PDECs (cases 3, 5, 10, 13, 18, 29, 34, and 35 in Table 1) using a panel of alpha-satellite DNA probes specific for chromosomes 1, 3, 6, 11, 17, and 18 and a probe specific for the *p53* gene on 17p13. The selection of the cases for FISH analysis was based on the tumor allelotypes to include both high FAI (cases 3, 5, 10, 13, and 18) and low FAI PDECs (cases 29, 34, and 35). Interphasic FISH was done according to the protocol reported by Chin et al. (24). The alpha-satellite probes for chromosomes 1 (D1Z1), 3 (D3Z1), 6 (D6Z1), 11 (D11Z1), 17 (D17Z1), 18 (D18Z1) labeled with Spectrum Orange or with Spectrum Green (CEP, Vysis, Abbot Diagnostics, Wiesbaden-Delkenheim, Germany) were used to evaluate chromosome aneusomy. The chromosome 17p13(*p53*)/alpha-satellite 17 cocktail dual color–labeled probe (Q-biogene, Illkirch Cedex, France) was used for the detection of copy numbers of the *p53* gene.

FISH signals were counted with a Leica DMRA microscope equipped with single- and triple-band pass filters. Images for documentation were captured using a Hamamatsu Chilled CCD Camera and processed by the Image ProPlus software (Immagini e Computer, Milan, Italy).

To ensure a representative sample and to permit an assessment of the extent of tumoral heterogeneity, the hybridization signals for each probe were counted in 200 to 300 interphasic nuclei from at least three separate areas of the tumor selected for well-preserved cellular and nuclear morphology. The total percentage of nuclei containing 1, 2, 3, 4, and ≥4 signals was determined for each chromosome using the criteria reported by Celep et al. (25).

Table 2 Microsatellite loci used for the allelotyping analysis

Cytogenetic regions	Microsatellite markers
1p	*D1S189; D1S440*
1q	*D1S2842; D1S249*
3p26-p25	*D3S1038; D3S1293*
3p21-p14	*D3S1606; D3S1295; D3S1300; D3S1581*
3q	*D3S1614; D3S1580*
4p	*D4S2994*
4q	*D4S392; D4S402*
5p	*D5S417; D5S407*
5q21-q22	*APC; D5S2049*
6p	*D6S470; D6S1610*
6q21-q22	*D6S268; D6S261; D6S1639*
6q25	*D6S441; D6S415*
6q27	*D6S193; D6S297*
7p	*D7S484; D7S507*
7q	*D7S2459*
8p	*D8S1820; D8S264*
8q	*D8S1720; D8S543*
10p	*D10S197; D10S1745*
10q	*D10S217; D10S580*
11p15	*D11S922; D11S1318; D11S4088; D11S4181*
11q13	*PYGM; INT2*
11q14-q22	*D11S917; D11S1339; D11S927; D11S1347*
17p13.2	*TP53*
17q	*D17S787; D17S928*
18p	*D18S63; D18S452*
18q21	*D18S363; D18S474; D18S70*

Some artifactual gain and loss is to be expected when working on paraffin-embedded tissues, even in normal tissue. Therefore, a total of 10 histologically normal specimens from the lung, stomach, colon, and reactive lymph nodes were analyzed and the results obtained were used to establish the cutoff values for the definition of true gain and loss in tumor samples (one-tailed 99% upper tolerance limit). The cutoff values for chromosome loss (monosomy) pertaining to chromosomes 1, 3, 6, 11, 17, and 18 were 24.8%, 33.3%, 45.1%, 15.1%, 35.5%, and 28.4%, respectively. The cutoff values for chromosome gain pertaining to chromosomes 1, 3, 6, 11, 17, and 18 were 6.1%, 6.6%, 1.8%, 11.2%, 2.1%, and 7.3%, respectively, for trisomy and 0% for all chromosomes for tetrasomy and hypertetrasomy. We increased the cutoff value for tetrasomy and hypertetrasomy to 1% for all chromosomes to avoid misinterpretation. After defining the cutoff values, the following criteria were used to classify the tumor samples: (a) an abnormal monosomy, trisomy, tetrasomy, or hypertetrasomy required a percentage of nuclei showing one, three, four, and more than four signals greater than or equal to the defined cutoff level; (b) a tumor was classified as aneuploid if at least one abnormal monosomy or trisomy or tetrasomy was found at one or more chromosomes; (c) a tumor was classified as triploid (tetraploid) if the autosomal average of the percentage of nuclei with three (four) signals was ≥10% (25, 26).

Statistical Analysis. The statistical analysis was done using Fisher's exact test, the χ^2 test with Yates' correction, the

independent sample *t* test, and the correlation analysis (SPSS 7.5 software).

The survival analysis was done by employing the Kaplan-Meier product limit estimate of probability of survival against time, producing a product limit survival curve for each of the following variables: size of the primary tumor, presence of metastases, tumor necrosis, Ki67 index, mitotic index, and percentage of allelic imbalance. For each survival curve, the relative risk of failure associated with being in the poor prognostic group and the results of the standard Mantel Haenzel log-rank test were calculated. For all the survival analyses, the program Survan XL, version 1.14 (copyright 1995-1997) was employed.

RESULTS

Clinicopathologic Findings. The group of patients consisted of 26 men and 10 women, with a mean age of 64.4 years (range, 37-86). The PDECs were located in the lung in six cases; the stomach in seven; the colon-rectum in 10; the bladder in three; the esophagus, the prostate, and the skin in two cases each; and the gallbladder, the pancreas, the endometrium, and the parotid gland in one case each. The stage of the disease was determined in 31 cases in which the clinical record was complete. Six tumors were confined to the primary site (stage I), 16 had loco-regional lymph node metastases (stage II) and nine had hematogenous metastases to the liver or lung (stage III). The mean size of the tumors was 4.6 cm (range, 0.4-14 cm).

Microscopically, all the tumors were composed of highly atypical cells growing in solid nests or, more rarely, in sheets. Cell size was small in seven tumors, intermediate in 26 (with scattered large cells in nine of these tumors) and large in three. Areas of necrosis were observed in 28 PDECs, ranging from <10% (+) to 10% to 30% (++) to >30% (+++) of the tumor mass. Invasion of vascular spaces was found in all tumors except one Merkel cell carcinoma of 0.8 cm in size. The mean number of mitoses was 101.5 × 10 high-power field (range, 33-219) and the mean Ki67 index was 55.5% (range, 15-71%).

It is of note that none of the clinicopathologic variables considered was related to the primary site of the PDECs, as none of the statistical tests gave significant results.

Molecular and Cytogenetic Profiles of Poorly Differentiated Endocrine Carcinomas. Fifty-seven microsatellite markers covering a total of 11 autosomes were investigated in a series of PDECs using standardized fluorescence-based methodology and apparatus. The comprehensive results of the allelotyping analysis together with the FAI of each tumor and the percentage of AI at each chromosome region are shown in Fig. 1.

The molecular profiles of PDECs showed a high degree of AI often involving extensive regions of the chromosome or entire chromosomes. The average FAI was 0.49, but a significantly higher mean FAI was observed among PDECs of the lung, esophagus, stomach, pancreas, parotid gland, and prostate compared with PDECs of the colon-rectum, gallbladder, bladder, endometrium, and skin (0.61 *versus* 0.36; $P < 0.001$). Very low FAI values (range, 0-0.25) were observed in only five cases including two Merkel cell carcinomas, one colorectal, one bladder and one endometrial PDEC (cases 34, 35, 15, 29, and 33, respectively, in Fig. 1).

Interphasic FISH for the autosomes 1, 3, 6, 11, 17, and 18 showed numerical aberrations of one or more chromosomes in all eight PDECs analyzed (cases 3, 5, 10, 13, 18, 29, 34, and 35 in Fig. 1). These cases were selected with the aim of confirming the allelotyping study and included PDECs exhibiting both high FAI values (cases 3, 5, 10, 13, and 18) and very low FAI values (cases 29, 34, and 35). The comprehensive results of the FISH analysis are shown in Fig. 2.

Aneuploidies were found in 77% of the overall analysis with a higher frequency of gains than losses (68% *versus* 32%). According to the criteria reported in Materials and Methods, four cases were aneuploid whereas three cases were triploid and one case exhibited the presence of both triploid and tetraploid cell populations. Looking at the relationship between the interphasic cytogenetic profiles and allelotypes of these tumors, the high-FAI PDEC group showed multiple aneusomies for all chromosomes, with a higher frequency of gains than losses (86% *versus* 14% of the total aneusomies observed). By contrast, the three cases with low-FAI values showed a significantly lower degree of numerical alterations than high-FAI tumors ($P = 0.00012$). Moreover, in the low-FAI group, the aneusomies were always represented by chromosome losses and no gains were observed (Fig. 2). Intriguingly, in this second group of low-FAI tumors the concordance between FISH and allelotyping results at specific chromosomes was very good whereas, among the high-FAI PDECs, AI at specific autosomes did not necessarily correspond to numerical chromosome abnormality detected by FISH or *vice versa*.

Chromosomal Regions Commonly Involved in Poorly Differentiated Endocrine Carcinomas. Regardless of the primary site, PDECs invariably showed AI at the *TP53* locus (17p13.2); this was the single most ubiquitous alteration observed in this study, being found in 31 of the 35 informative PDECs (89%). Moreover, all tumors exhibiting *TP53* AI always showed the most significant allelic imbalance factors at this locus with respect to the remaining microsatellite markers investigated for that tumor.

The immunohistochemical analysis for p53 confirmed the AI results in 22 of the 31 cases (71%) in which both the analyses were done. In particular, an immunohistochemical protein accumulation was observed in 18 of 27 (67%) PDECs with *TP53* AI and no immunoreactivity was observed for all four cases without AI at this locus. The remaining nine cases of 31 (29%) showed *TP53* AI but no immunohistochemical p53 accumulation.

Furthermore, to enumerate the copy number of the *p53* gene with respect to the ploidy level of chromosome 17, FISH experiments were carried out using a chromosome 17p13(*p53*)/alpha-satellite 17 cocktail dual color–labeled probe in the same panel of eight PDECs reported in Fig. 2. Scoring FISH signals for chromosome 17 and for the *p53* gene, a loss of at least one copy of *p53* was observed in all PDECs regardless of the ploidy and the genetic heterogeneity of chromosome 17 aneusomies. The percentage of cells with *p53* loss in each tumor cell line relative to the ploidy level inferred with alpha-satellite for chromosome 17, the allelotype at the TP53 locus and the immunoreactivity for p53 are summarized in Fig. 3. In detail, the presence of *TP53* AI was observed in seven of the eight PDECs, with a complete signal reduction of one allele in six cases. This result is indicative of the success of the enrichment for

neoplastic cellularity but also of the clonal fixation of this genetic alteration. Among these cases, FISH analysis showed that the percentage of cells with *p53* loss increased with the ploidy level of chromosome 17. The only exception was case 3, that showed a complete allelic imbalance at the *TP53* locus in the presence of a very low fraction of trisomic cells for chromosome 17 as well as a low percentage of *p53* loss in the disomic cells of the autosome.

The only PDEC without *TP53* AI (case 34) was a Merkel cell carcinoma exhibiting only a disomic cell line for chromosome 17 and a loss of *p53* in 31.3% of these cells. This result underlines the technical limit of the allelotyping analysis in the detection of alterations affecting only a fraction of tumor cells before the clonal fixation.

On the whole, loss of *p53* shown in all cases by AI and/or FISH analyses was confirmed by immunohistochemistry as abnormal p53 accumulation in only 50% of these tumors (Fig. 3).

Besides the widespread involvement of the *TP53* locus in AI, at least two other chromosomal regions seemed to be involved in all PDECs, irrespective of the primary site and the clinicopathologic profile of the tumors. In particular, considering the chromosomal regions exhibiting an AI % higher than the mean AI % + 1SD calculated for the total series (65%), the chromosome arms 18q and 10q stood out among the other chromosome regions (72 and 68 AI % respectively).

Site-Specific Genetic Alterations and Molecular Markers Assisting in the Diagnosis of Lung Poorly Differentiated Endocrine Carcinomas. Despite the presence of the common genetic alterations reported above, some differences in allelotypes were observed in relation to the primary site of the tumors. In particular, considering the three most represented sites in this study, lung PDECs invariably showed AI on chromosomes 3p, 5, and 11q13, gastric PDECs were notable for the recurrent involvement of chromosomes 7 and 11q22 and colorectal PDECs for frequent AI at chromosomes 5q21, 8p, and 18q. According to these results, we observed that the concurrent detection of AI at chromosome region 3p14-p26 and at chromosome 5 may aid the diagnosis of primary PDECs of the lung with a sensitivity of 100%,

	Lung							Stomach								Colon-rectum												ES		P	G	Bladder			Pros		E	Skin		P*	Total series
	1	2	3	4	5	6	**AI%**	7	8	9	10	11	12	13	**AI%**	14	15	16	17	18	19	20	21	22	23	**AI%**	24	25	26	27	28	29	30	31	32	33	34	35	36	**AI%**
1p							33								29											10											-			29
1q							17					na			50							-	-			50		-	-											39
3p26-p25							**100**					-		-	20	-										22														45
3p21-p14				-			**100**								57											20					na					-			na	50
3q							50	-	-						20		na				-	-				43				-				-						34
4p							67		na		-			-	75			-					-			38	-			-									-	43
4q	na	-			-		33		-			na		-	75			na		na						38						-		na			-	na	46
5p							**100**	na	-						60	-	-	-				na				67								-					-	55
5q21-q22			-				**100**								43			na								**89**	-													64
6p							33			-		-			80			-								56				-	-									48
6q21-q22						-	0								57											30														40
6q25							17								57											30											-			49
6q27		-	-	na		-	0							-	50				-			-	-	-		33					-	-					-			46
7p	na	na					25		-						**83**	-										44													-	45
7q				-	-	-	33					-			**83**											40	-	na						na	-			na	44
8p							50	na	na						60											**60**					-								52
8q				na			60		na						67			-			-					50						-					-			57
10p	na						40	-	-		-		na		33	-		-				na			-	33		-		-						-		na	35
10q	na					-	75		na						**83**		na					-	-			57		-			na	na					-	-	**68**
11p15							33								57											20														36
11q13					-		**100**								71											30										-				53
11q14-q22							67								**86**											30														53
17p13.2		■	■	■	■		**100**		■	■		■			**100**	■	⊠	■		■	■	-	■		⊠	**78**		■		⊠	■		■	⊠		■		■	■	**89**
17q			-				20								57				na						-	50	-		-						-						40
18p				na			40	-				-			60			-								22		-	na											43
18q21							83								71											**60**														**72**
FAI (x100)	**45**	**65**	**83**	**52**	**30**	**55**	**55±18**	**71**	**59**	**48**	**54**	**50**	**64**	**86**	**62±13**	**32**	**13**	**44**	**29**	**64**	**42**	**42**	**45**	**44**	**58**	**41±14**	**77**	**62**	**78**	**36**	**57**	**14**	**50**	**71**	**36**	**25**	**0**	**21**	**78**	**49±21**

Fig. 1 Allelotypes of PDECs. Abbreviations: ES, Esophagus; P, Pancreas; G, Gallbladder; Pros, Prostate; E, Endometrium; P*, Parotid gland. Gray Box, AI; White box, allelic retention; –, no informative loci in the chromosomal region; na, not available results. In line 17p13.2, cases with presence (■) or absence (□) of p53 immunoreactive cells. Cases with not available results for p53 IIC (⊠). The AI columns indicate the percentage of AI for each chromosome regions, calculated by dividing the number of tumors that showed AI by the total number of informative cases for that particular region, among lung, gastric, colorectal PDECs, or the total series. For each tumor, the FAI was calculated by the number of chromosome regions having AI divided by the total number of informative chromosome regions. The mean FAI ± 1SD and the mean AI% ± 1SD were calculated for the lung, gastric, and colorectal PDECs and for the total series. The values of AI higher than the mean AI% + 1SD (86% lung, 81% stomach, 60% colon-rectum, and 65% total series) were indicated in bold.

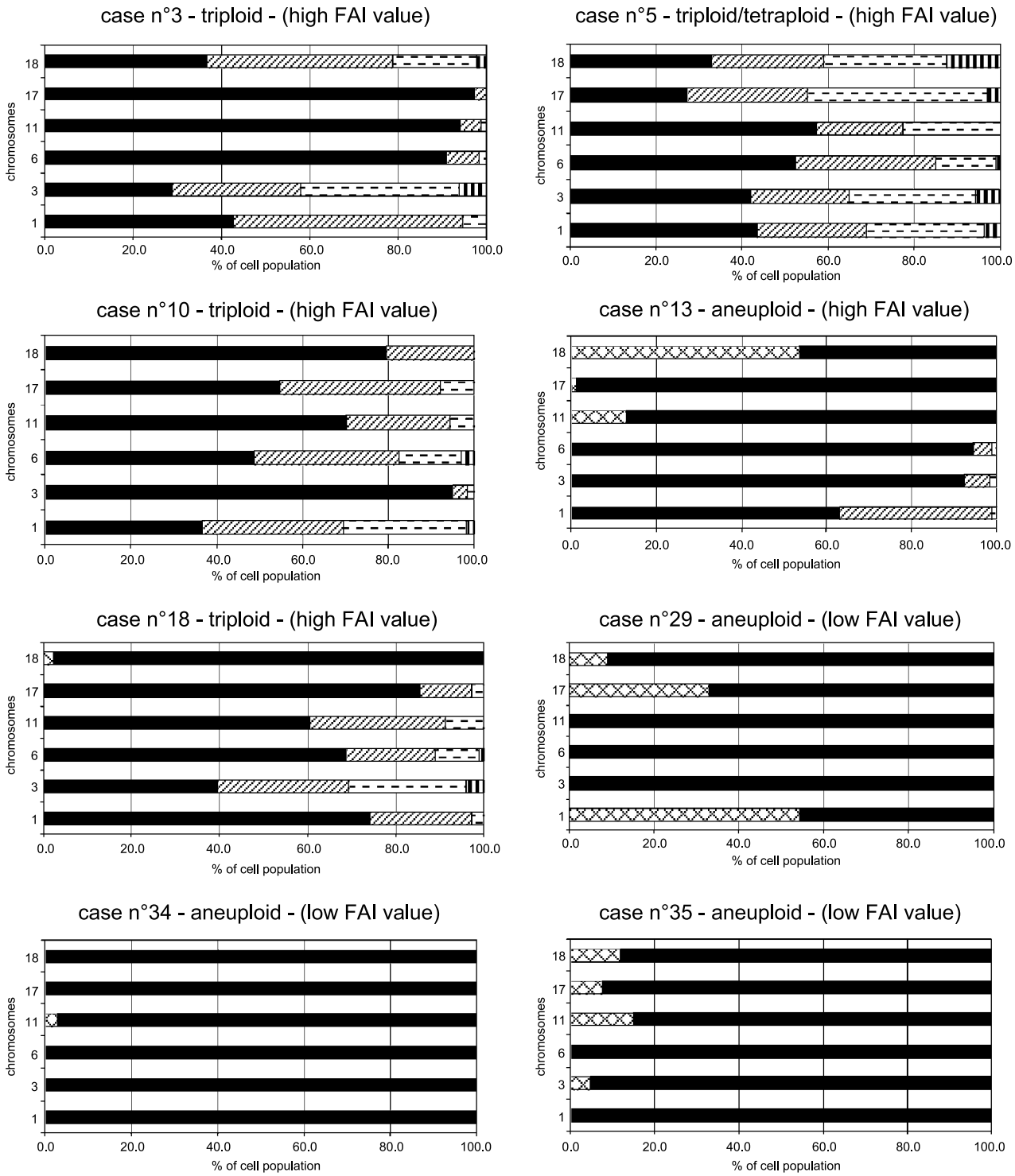

Fig. 2 Interphasic FISH for the autosomes 1, 3, 6, 11, 17, and 18 in selected PDECs. Percentage of cells with monosomy (⊠), disomy (■), trisomy (▨), tetrasomy (⊟), and hypertetrasomy (▥) for each of the six autosomes investigated. These percentages were obtained by subtracting the cutoff values reported in Materials and Methods from the raw percentages of tumor nuclei scored showing one, three, four, and more than four signals for each chromosome.

a specificity of 96.5%, a predictive value of 86% for a positive diagnosis, a predictive value of 100% for a negative diagnosis and an overall accuracy of 97.1%.

Univariate Analysis. Follow-up data were available for 34 of the 36 patients. One patient (case 4 in Table 1) died of a cause unrelated to the PDEC. Twenty-two patients (67 %) died

Case N^0	Loss of p53 relative to the ploidy level of chr 17	Allelic imbalance at TP53 locus	% of cells with IIC p53 accumulation
34 (low FAI)	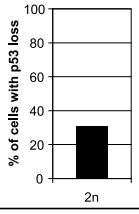	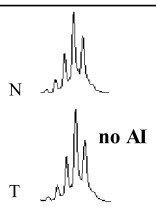	0
29 (low FAI)	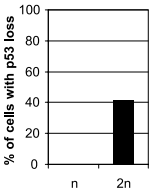	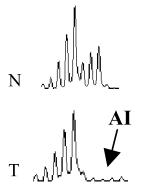	0
35 (low FAI)	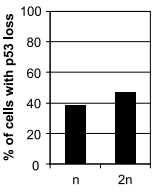	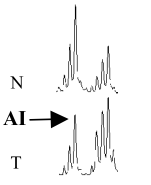	80
13 (high FAI)	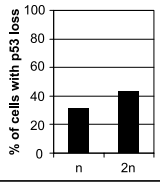	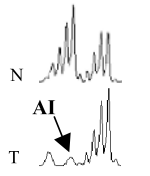	0
3 (high FAI)	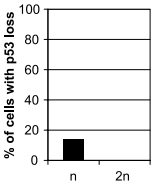	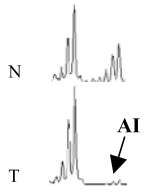	70
10 (high FAI)	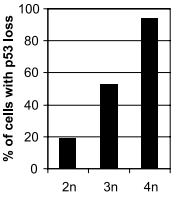	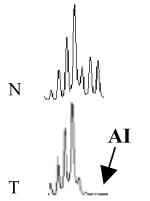	0
18 (high FAI)	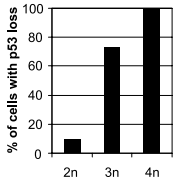	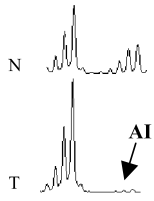	80
5 (high FAI)	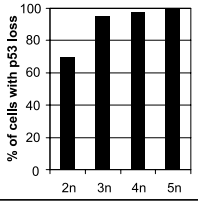	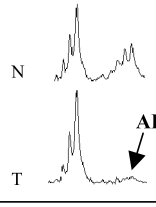	60

Fig. 3 *TP53* gene status according to FISH, molecular, and immunohistochemical analyses in both low- and high-FAI PDECs.

of disease after a median time of 5 months (range, 1-28), whereas 11 patients (33%) were living after a median follow-up time of 22 months (range, 8-72). We did not find any correlation between clinicopathologic variables (tumor size, stage, presence of metastases, necrosis, cell size, number of mitosis, and Ki67 index) and patient outcome. The only significant prognostic factor was the skin as the primary site of the PDEC, as the good prognosis of Merkel cell carcinoma is well known.

Although very low FAI values (range, 0-0.25) were observed in only five cases [two Merkel cell carcinomas (cases 34 and 35), one colorectal (case 15), one bladder (case 29) and one endometrial (case 33) PDECs], a low percentage of AI seems to be associated with a longer survival (patients 15 and 29 died of disease after 1 and 23 months, whereas patients 33, 34, and 35 are alive with no evidence of disease after 39, 29, and 38 months, respectively).

Furthermore, the AI status at three chromosome regions was related to patient outcome. In particular, significantly better outcome was observed in patients with PDECs exhibiting (a) the presence of AI at chromosome 8q or (b) the absence of AI at chromosome 6p or (c) the absence of AI at chromosome region 6q25 (Fig. 4).

DISCUSSION

In the present study, we compared the allelotypes of 36 PDECs of different sites, including the lung, the esophagus, parotid gland, stomach, pancreas, gallbladder, colon-rectum, bladder, prostate, endometrium, and skin. Given the rarity of these tumors, this panel of extrapulmonary PDECs, the morphofunctional profiles of which were carefully reviewed according to WHO criteria (1, 2), represents the largest series thus far examined by molecular approaches.

The allelotyping analysis covering 11 autosomes with 57 fluorescent microsatellite markers showed that, regardless of the primary site, 31 of 36 (86%) PDECs exhibit very complex allelotypes with allelic imbalance involving extensive chromosome regions or entire chromosomes. These data strongly suggest an abnormal chromosomal content with multiple aneuploidies and/or chromosome rearrangements. Molecular findings about extrapulmonary PDECs are very scanty and fragmentary (9, 12–14, 27, 28); however, our results are largely consistent with the wealth of cytogenetic and molecular data showing very complex karyotypes in lung PDECs (16, 17). Although high FAI values were generally observed in our series, some heterogeneity among the different sites was noted. In particular, we found significantly higher mean FAI among PDECs of the lung, esophagus, stomach, pancreas, parotid gland, and prostate compared with PDECs of the colon and rectum, gallbladder, bladder, endometrium, and skin (Fig. 1). Intriguingly, the lowest FAI values were detected in five cases for which an overall longer survival was observed. In particular, these cases included two Merkel cell carcinomas known from the literature to be less aggressive PDECs (29).

These data suggest that, also among PDECs known to be a fatal disease, the percentage of chromosomal abnormalities as well as the ploidy status could be used as markers of potential prognostic value, as reported for other tumors (30–32). In this connection, some authors have very recently suggested that significant differences in survival may exist among patients with PDECs. In particular, Jones et al. used a cDNA microarray expression analysis to divide a panel of 38 lung PDECs into two prognostically significant subtypes (33). Other investigators showed that the immunohistochemical expression of cytokeratin 20 can be used to classify PDECs of the parotid gland into Merkel cell and pulmonary types and this classification may have prognostic significance (33, 34).

Interphasic FISH with centromeric probes added important information about the abnormal chromosomal content shown by the allelotyping analysis of the PDECs in this study. This analysis has proven to be extremely useful in distinguishing a state of aneuploidy (an abnormal chromosomal content reflected in allelic imbalance at the molecular level), from a condition of chromosomal instability (an accelerated rate of gains or losses of whole or large portions of chromosomes; ref. 35). Although the FISH approach does not directly measure an increased rate of aberrations, the chromosomal heterogeneity detectable by this analysis may serve as a good indicator of CIN (36). On the other hand, an allelotyping analysis, like all techniques that pool DNA, cannot provide information about CIN. In the present work, a high grade of chromosomal heterogeneity suggestive of a CIN phenotype was observed in all the high-FAI PDECs. In contrast, the panel of three cases with low FAI allelotypes showed aneuploidies in the absence of a CIN phenotype. Intriguingly, the aneusomies observed in these PDECs were always represented by chromosome losses, whereas chromosome gains were consistently detected in the five CIN PDECs. These findings are in broad agreement with the extensive cytogenetic and molecular data showing that the loss of a specific chromosome represents one step in the inactivation of a tumor suppressor gene residing on the lost chromosome and that this genetic event frequently marks an early phase of carcinogenesis (37).

Careful observation of the cytogenetic and molecular profiles of these eight PDECs highlighted the noteworthy finding that *p53* loss is the only genetic alteration of both PDECs with minimal cytogenetic/molecular anomalies and CIN PDECs (Figs. 1-3). Therefore, the second important result of our work is the demonstration of a very early involvement of p53 in the pathogenesis of PDECs. Although it is not clear if the inactivation of p53 is causally related to the acquisition of aneuploidies and/or CIN in these tumors, our data strongly support an early and clonal selection of p53 alterations during the progression of these tumors. This conclusion is sustained by at least five different observations: (a) the allelotyping analysis showed that *TP53* AI is a widespread alteration in PDECs regardless of the stage or the primary site of the tumor; (b) a complete signal reduction of one allele was observed in almost all PDECs, suggesting the clonal fixation of this alteration in the whole tumor population; (c) the most significant AI factor was invariably observed at the *TP53* locus rather than the other loci, suggesting the early involvement of the 17p13 region in the pathogenesis of PDECs; (d) in low FAI PDECs, FISH analysis clearly showed loss of the *p53* gene and/or loss of chromosome 17 affecting a subpopulation of the tumor cells before the clonal fixation (case 34 in Fig. 3) or involving such a large proportion of cancer cells as to be detected as a clonal event by the allelotyping analysis (cases 35 and 13 in Fig. 3); (e) in three high FAI cases (10, 18, and 5 in Fig. 3) FISH analysis showed a concurrent increase in the cell fractions exhibiting *p53*

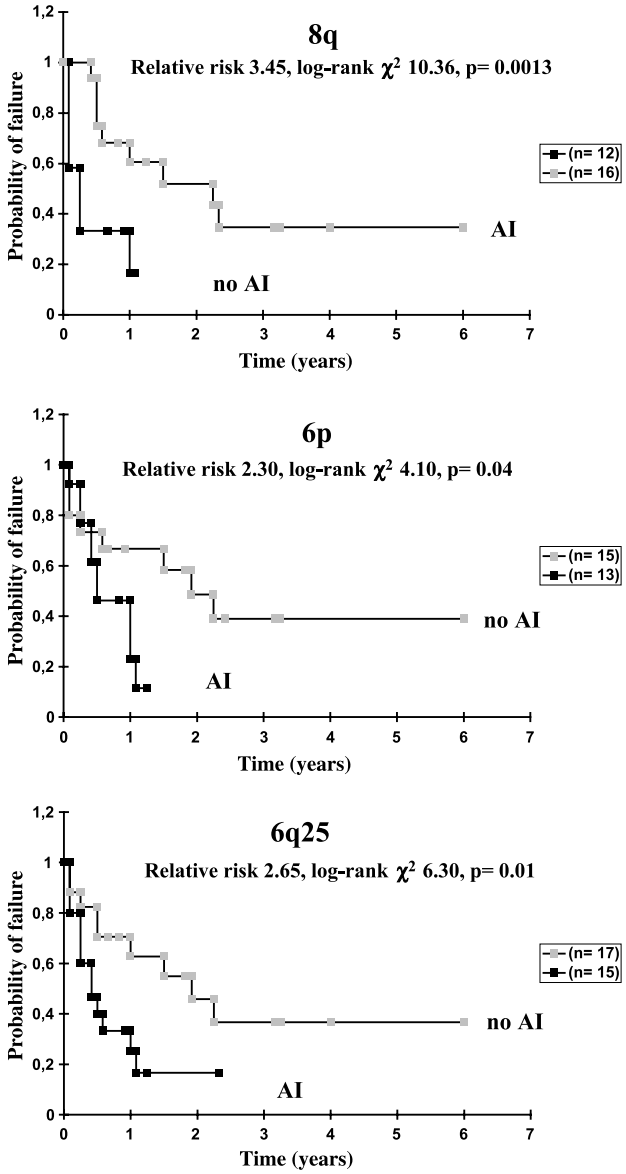

Fig. 4 Failure time according to AI status at chromosomes 8q, 6p, and 6q25.

loss with the ploidy of chromosome 17. Intriguingly, case 3 showed a complete allelic imbalance at the *TP53* locus in the presence of a very low fraction of triploid cells for chromosome 17 as well as a low percentage of *p53* loss in the disomic cells of the autosome. These results strongly indicate a reduplication event for chromosome 17 (i.e., the loss of chromosome 17 followed by a duplication of the remaining autosome), leaving in a cell a normal chromosome copy number, detectable by FISH analysis, even when AI is present.

Such reduplication might be necessary to protect the cell from death due to haploinsufficiency (38, 39). Despite these countermeasures through dosage compensation, loss of expression of the p53 protein might be a frequent event in PDECs, as we observed a high percentage of PDECs (29%) showing *TP53* AI but no abnormal immunohistochemical accumulation of the protein.

Overall these results confirm that the concurrence of p53 inactivation and aneuploidies or CIN are the main features of PDECs. Although this association has been frequently observed in solid tumors leading to the hypothesis that p53 may actively repress CIN (40, 41), several investigators have recently shown that abrogation of p53 function is not a prerequisite for CIN in diploid human cell lines. Thus, other mechanisms may directly cause chromosome missegregation including centrosomal abnormalities (42–44), inappropriate chromosome condensation or cohesion, deregulated mitotic progression, an impairment of the spindle-assembly checkpoint, cytokinesis malfunction, endoreduplication, or cell fusion (45–48).

In agreement with this hypothesis, Wistuba et al. recently showed that the microdissected epithelial cells of histologically normal bronchial mucosa accompanying small cell lung cancers exhibit extensive genetic damage even in the absence of p53 inactivation (49). The authors suggest that in small cell lung cancer, in which no characteristic preneoplastic sequence of morphologic changes has been described, the tumors may arise quickly and directly from either normal or hyperplastic epithelia. In this scenario, it is plausible to think that a number of cellular stresses, such as cell crowding, hypoxia, acidity, or inflammation, may induce a strong selection pressure specifically against the apoptotic function of p53. Indeed, hypoxia is the main physiologic inducer of p53 and it is likely that cells lacking p53 may have a selective advantage in such an environment (50, 51). Hypoxia is surely a common event in PDECs of all sites, as indicated by the multiple necrotic regions commonly found in these tumors, and it probably plays an essential role both in mediating the strong selection of cellular clones with p53 loss and in determining the invasive and metastatic potential that marks these tumors (52–55).

This model could explain additional findings obtained in our work, concerning the distinct genetic alterations observed in PDECs in relation to the primary sites. In this connection, our study showed that despite the similarity in histologic appearance, PDECs display molecular anomalies known to be crucial in the pathogenesis of the exocrine tumors of the same sites. In particular, we observed recurrent allelic imbalances on 3p, 5, and 11q13 in lung PDECs, on 5q21, 8p, and 18q in colorectal PDECs and on 7 and 11q22 in gastric PDECs. Because of the well-known involvement of these chromosome regions in the exocrine tumorigenesis of each site (17, 21, 22, 56), our work strongly supports the hypothesis that PDECs and exocrine carcinomas of all sites may share both their histogenesis and early pathogenetic mechanisms. This model may explain the existence of rare pulmonary and extrapulmonary mixed exocrine/endocrine tumors where an adenomatous and/or carcinomatous component is associated with a PDEC. In these mixed tumors, a close genetic relationship between the endocrine and the exocrine components has been shown, supporting the hypothesis of a common pathogenetic mechanism between PDECs and carcinomas of the same site (9–11).

An additional finding of this work concerns the identification of molecular markers of potential diagnostic and prognostic values for PDECs of different sites. In particular, we suggested the diagnostic relevance of the concurrent detection of AI at chromosome region 3p14-p26 and at chromosome 5 in assisting in the diagnosis of primary PDEC of the lung. Moreover, we

showed the prognostic relevance of the AI status at chromosome regions 8q, 6p, and 6q25 in predicting the survival of these patients. Further studies that include greater number of these neoplasms would be helpful in defining the reliability of the molecular markers identified in this work.

ACKNOWLEDGMENTS

We thank Centro Grandi Strumenti of the University of Insubria for the instruments used in this study.

REFERENCES

1. Solcia E, Kloppel G, Sobin LH. Histological typing of endocrine tumours. World Health Organization international histological classification of tumours. Berlin Heidelberg: Springer Verlag; 2000.

2. Brambilla E, Travis WD, Colby TV, Corrin B, Shimosato Y. The new World Health Organization classification of lung tumours. Eur Respir J 2001;18:1059–68.

3. Remick SC, Ruckdeschel JC. Extrapulmonary and pulmonary small-cell carcinoma: tumor biology, therapy, and outcome. Med Pediatr Oncol 1992;20:89–99.

4. Richardson RL, Weiland LH. Undifferentiated small cell carcinomas in extrapulmonary sites. Semin Oncol 1982;9:484–96.

5. Ibrahim NB, Briggs JC, Corbishley CM. Extrapulmonary oat cell carcinoma. Cancer 1984;54:1645–61.

6. Galanis E, Frytak S, Lloyd RV. Extrapulmonary small cell carcinoma. Cancer 1997;79:1729–36.

7. Shamelian SO, Nortier JW. Extrapulmonary small-cell carcinoma: report of three cases and update of therapy and prognosis. Neth J Med 2000;56:51–5.

8. Ihde D, Souhami B, Comis R, et al. Small cell lung cancer. Lung Cancer 1997;17 Suppl 1:S19–21.

9. Vortmeyer AO, Lubensky IA, Merino MJ, et al. Concordance of genetic alterations in poorly differentiated colorectal neuroendocrine carcinomas and associated adenocarcinomas. J Natl Cancer Inst 1997;89:1448–53.

10. Kim KM, Kim MJ, Cho BK, Choi SW, Rhyu MG. Genetic evidence for the multi-step progression of mixed glandular-neuroendocrine gastric carcinomas. Virchows Arch 2002;440:85–93.

11. Furlan D, Cerutti R, Genasetti A, et al. Microallelotyping defines the monoclonal or the polyclonal origin of mixed and collision endocrine-exocrine tumors of the gut. Lab Invest 2003;83:963–71.

12. Dacic S, Finkelstein SD, Baksh FK, Swalsky PA, Barnes LE, Yousem SA. Small-cell neuroendocrine carcinoma displays unique profiles of tumor-suppressor gene loss in relationship to the primary site of formation. Hum Pathol 2002;33:927–32.

13. Pizzi S, Azzoni C, Bassi D, Bottarelli L, Milione M, Bordi C. Genetic alterations in poorly differentiated endocrine carcinomas of the gastrointestinal tract. Cancer 2003;98:1273–82.

14. Furlan D, Cerutti R, Uccella S, et al. Different molecular profiles characterize well-differentiated endocrine tumors and poorly differentiated endocrine carcinomas of the gastroenteropancreatic tract. Clin Cancer Res 2004;10:947–57.

15. Michelland S, Gazzeri S, Brambilla E, Robert-Nicoud M. Comparison of chromosomal imbalances in neuroendocrine and non-small-cell lung carcinomas. Cancer Genet Cytogenet 1999;114:22–30.

16. Masuda A, Takahashi T. Chromosome instability in human lung cancers: possible underlying mechanisms and potential consequences in the pathogenesis. Oncogene 2002;21:6884–97.

17. Wistuba, II, Gazdar AF, Minna JD. Molecular genetics of small cell lung carcinoma. Semin Oncol 2001;28:3–13.

18. Wistuba, II, Mao L, Gazdar AF. Smoking molecular damage in bronchial epithelium. Oncogene 2002;21:7298–306.

19. Zabarovsky ER, Lerman MI, Minna JD. Tumor suppressor genes on chromosome 3p involved in the pathogenesis of lung and other cancers. Oncogene 2002;21:6915–35.

20. Johnson BE, Whang-Peng J, Naylor SL, et al. Retention of chromosome 3 in extrapulmonary small cell cancer shown by molecular and cytogenetic studies. J Natl Cancer Inst 1989;81:1223–8.

21. Testa JR, Liu Z, Feder M, et al. Advances in the analysis of chromosome alterations in human lung carcinomas. Cancer Genet Cytogenet 1997;95:20–32.

22. Vogelstein B, Kinzler KW. The genetic basis of human cancer. New York: McGraw-Hill; 1998. p. 565–87.

23. Yuasa Y. Control of gut differentiation and intestinal-type gastric carcinogenesis. Nat Rev Cancer 2003;3:592–600.

24. Chin SF, Daigo Y, Huang HE, et al. A simple and reliable pretreatment protocol facilitates fluorescent *in situ* hybridisation on tissue microarrays of paraffin wax embedded tumour samples. Mol Pathol 2003;56:275–9.

25. Celep F, Karaguzel A, Ozgur GK, Yildiz K. Detection of chromosomal aberrations in prostate cancer by fluorescence *in situ* hybridization (FISH). Eur Urol 2003;44:666–71.

26. Takahashi S, Alcaraz A, Brown JA, et al. Aneusomies of chromosomes 8 and Y detected by fluorescence *in situ* hybridization are prognostic markers for pathological stage C (pt3N0M0) prostate carcinoma. Clin Cancer Res 1996;2:137–45.

27. Han HS, Kim HS, Woo DK, Kim WH, Kim YI. Loss of heterozygosity in gastric neuroendocrine tumor. Anticancer Res 2000;20:2849–54.

28. D'Adda T, Keller G, Bordi C, Hofler H. Loss of heterozygosity in 11q13-14 regions in gastric neuroendocrine tumors not associated with multiple endocrine neoplasia type 1 syndrome. Lab Invest 1999;79:671–7.

29. Sibley RK DL, Rosai J. Primary neuroendocrine (Merkel cell?) carcinoma of the skin. I. A clinicopathologic and ultrastructural study of 43 cases. Am J Surg Pathol 1985;9:95–108.

30. Evans MP, Podratz KC. Endometrial neoplasia: prognostic significance of ploidy status. Clin Obstet Gynecol 1996;39:696–706.

31. von Rosen A, Rutqvist LE, Carstensen J, Fallenius A, Skoog L, Auer G. Prognostic value of nuclear DNA content in breast cancer in relation to tumor size, nodal status, and estrogen receptor content. Breast Cancer Res Treat 1989;13:23–32.

32. Berek JS, Martinez-Maza O, Hamilton T, et al. Molecular and biological factors in the pathogenesis of ovarian cancer. Ann Oncol 1993;4 Suppl 4:3–16.

33. Jones MH, Virtanen C, Honjoh D, et al. Two prognostically significant subtypes of high-grade lung neuroendocrine tumours independent of small-cell and large-cell neuroendocrine carcinomas identified by gene expression profiles. Lancet 2004;363:775–81.

34. Nagao T, Gaffey TA, Olsen KD, Serizawa H, Lewis JE. Small cell carcinoma of the major salivary glands: clinicopathologic study with emphasis on cytokeratin 20 immunoreactivity and clinical outcome. Am J Surg Pathol 2004;28:762–70.

35. Rajagopalan H, Nowak MA, Vogelstein B, Lengauer C. The significance of unstable chromosomes in colorectal cancer. Nat Rev Cancer 2003;3:695–701.

36. Wilkens L, Flemming P, Gebel M, et al. Induction of aneuploidy by increasing chromosomal instability during dedifferentiation of hepatocellular carcinoma. Proc Natl Acad Sci U S A 2004;101:1309–14.

37. Muleris M, Salmon RJ, Zafrani B, Girodet J, Dutrillaux B. Consistent deficiencies of chromosome 18 and of the short arm of chromosome 17 in eleven cases of human large bowel cancer: a possible recessive determinism. Ann Genet 1985;28:206–13.

38. Brat DJ, Hahn SA, Griffin CA, Yeo CJ, Kern SE, Hruban RH. The structural basis of molecular genetic deletions. An integration of classical cytogenetic and molecular analyses in pancreatic adenocarcinoma. Am J Pathol 1997;150:383–91.

39. Thiagalingam S, Laken S, Willson JK, et al. Mechanisms underlying losses of heterozygosity in human colorectal cancers. Proc Natl Acad Sci U S A 2001;98:2698–702.

40. Harvey M, Sands AT, Weiss RS, et al. *In vitro* growth characteristics of embryo fibroblasts isolated from p53-deficient mice. Oncogene 1993;8:2457–67.

41. Campomenosi P, Assereto P, Bogliolo M, et al. p53 mutations and DNA ploidy in colorectal adenocarcinomas. Anal Cell Pathol 1998;17:1–12.

42. Pihan GA, Doxsey SJ. The mitotic machinery as a source of genetic instability in cancer. Semin Cancer Biol 1999;9:289–302.

43. Lingle WL, Salisbury JL. The role of the centrosome in the development of malignant tumors. Curr Top Dev Biol 2000;49:313–29.

44. Brinkley BR. Managing the centrosome numbers game: from chaos to stability in cancer cell division. Trends Cell Biol 2001;11:18–21.

45. Zhou H, Kuang J, Zhong L, et al. Tumour amplified kinase STK15/BTAK induces centrosome amplification, aneuploidy and transformation. Nat Genet 1998;20:189–93.

46. Hollander MC, Sheikh MS, Bulavin DV, et al. Genomic instability in Gadd45a-deficient mice. Nat Genet 1999;23:176–84.

47. Nakayama K, Nagahama H, Minamishima YA, et al. Targeted disruption of Skp2 results in accumulation of cyclin E and p27(Kip1), polyploidy and centrosome overduplication. Embo J 2000;19:2069–81.

48. Jallepalli PV, Lengauer C. Chromosome segregation and cancer: cutting through the mystery. Nat Rev Cancer 2001;1:109–17.

49. Wistuba, II, Berry J, Behrens C, et al. Molecular changes in the bronchial epithelium of patients with small cell lung cancer. Clin Cancer Res 2000;6:2604–10.

50. Graeber TG, Peterson JF, Tsai M, Monica K, Fornace AJ, Giaccia AJ. Hypoxia induces accumulation of p53 protein, but activation of a G_1-phase checkpoint by low-oxygen conditions is independent of p53 status. Mol Cell Biol 1994;14:6264–77.

51. Graeber TG, Osmanian C, Jacks T, et al. Hypoxia-mediated selection of cells with diminished apoptotic potential in solid tumours. Nature 1996;379:88–91.

52. Semenza GL. Hypoxia-inducible factor 1: master regulator of O2 homeostasis. Curr Opin Genet Dev 1998;8:588–94.

53. Page EL, Robitaille GA, Pouyssegur J, Richard DE. Induction of hypoxia-inducible factor-1α by transcriptional and translational mechanisms. J Biol Chem 2002;277:48403–9.

54. Pennacchietti S, Michieli P, Galluzzo M, Mazzone M, Giordano S, Comoglio PM. Hypoxia promotes invasive growth by transcriptional activation of the met protooncogene. Cancer Cell 2003;3:347–61.

55. Berra E, Benizri E, Ginouves A, Volmat V, Roux D, Pouyssegur J. HIF prolyl-hydroxylase 2 is the key oxygen sensor setting low steady-state levels of HIF-1α in normoxia. Embo J 2003;22:4082–90.

56. Baffa R, Negrini M, Mandes B, et al. Loss of heterozygosity for chromosome 11 in adenocarcinoma of the stomach. Cancer Res 1996;56:268–72.